TUTORIAL REVIEW

Ultrafast dynamics of single molecules

Daan Brinks,†[ab] Richard Hildner,†[ac] Erik M. H. P. van Dijk,[d] Fernando D. Stefani,[ae] Jana B. Nieder,[a] Jordi Hernando[f] and Niek F. van Hulst*[ag]

The detection of individual molecules has found widespread application in molecular biology, photo-chemistry, polymer chemistry, quantum optics and super-resolution microscopy. Tracking of an individual molecule in time has allowed identifying discrete molecular photodynamic steps, action of molecular motors, protein folding, diffusion, etc. down to the picosecond level. However, methods to study the ultrafast electronic and vibrational molecular dynamics at the level of individual molecules have emerged only recently. In this review we present several examples of femtosecond single molecule spectroscopy. Starting with basic pump–probe spectroscopy in a confocal detection scheme, we move towards deter-ministic coherent control approaches using pulse shapers and ultra-broad band laser systems. We present the detection of both electronic and vibrational femtosecond dynamics of individual fluorophores at room temperature, showing electronic (de)coherence, vibrational wavepacket interference and quantum control. Finally, two colour phase shaping applied to photosynthetic light-harvesting complexes is presented, which allows investigation of the persistent coherence in photosynthetic complexes under physiological conditions at the level of individual complexes.

Key learning points
(1) Strategies to acquire the femtosecond dynamic response of single molecules.
(2) Intramolecular vibrational relaxation of a single molecule.
(3) Electronic coherence and quantum control of individual molecules at room temperature.
(4) Vibrational wavepacket interference in a single molecule.
(5) Coherent electronic energy transfer of individual photosynthetic complexes at room temperature.

1. Introduction: motivation for femtosecond single-molecule detection

Over the last 25 years the optical detection of single molecules has developed tremendously.[1–4] Observing individual molecules one by one removes the usual ensemble averaging and enables the detection of the different subpopulations present in complex and heterogeneous systems (Fig. 1). Furthermore, following the behaviour of individual molecules in time, without the need to synchronize the ensemble, provides extensive insights into the dynamic behaviour of (bio-)molecules.[5] Individual molecules are influenced by their local environment, resulting in variations from molecule to molecule in their steady state absorption/emission spectra, transition dipole orientation, triplet and fluorescence lifetimes, etc.[6–9] Single molecule experiments consistently show that chemically identical molecules exhibit large spatial and temporal heterogeneity for all parameters studied.

The dynamic range of the processes that can be studied in conventional single molecule experiments is typically limited. Detecting the Stokes shifted fluorescence arising from an individual molecular system has proven to be the most straight-forward way to enable background free detection and discriminate the weak response of a single molecule from both the scattered irradiation field and the signal of the surrounding medium.[10] Indeed, using efficient photon counters, typically 10^2–10^5 counts per second are detected from a single fluorescent molecule. Fig. 2 shows the typical timescales of some of

[a] ICFO - Institut de Ciencies Fotoniques, Mediterranean Technology Park, 08860 Castelldefels, Barcelona, Spain. E-mail: Niek.vanHulst@ICFO.eu; Web: www.ICFO.eu
[b] Department of Chemistry and Chemical Biology, Harvard University, Cambridge, MA 02138, USA
[c] Experimentalphysik IV, Universität Bayreuth, 95440 Bayreuth, Germany
[d] Philips Healthcare, 5680DA Best, The Netherlands
[e] Depto. de Física, Universidad de Buenos Aires, 1438 Buenos Aires, Argentina
[f] Dept. de Química, Universitat Autònoma de Barcelona, 08193 Cerdanyola del Vallès, Barcelona, Spain
[g] ICREA - Institució Catalana de Recerca i Estudis Avançats, 08015 Barcelona, Spain
† Equal contribution.

This journal is © The Royal Society of Chemistry 2014

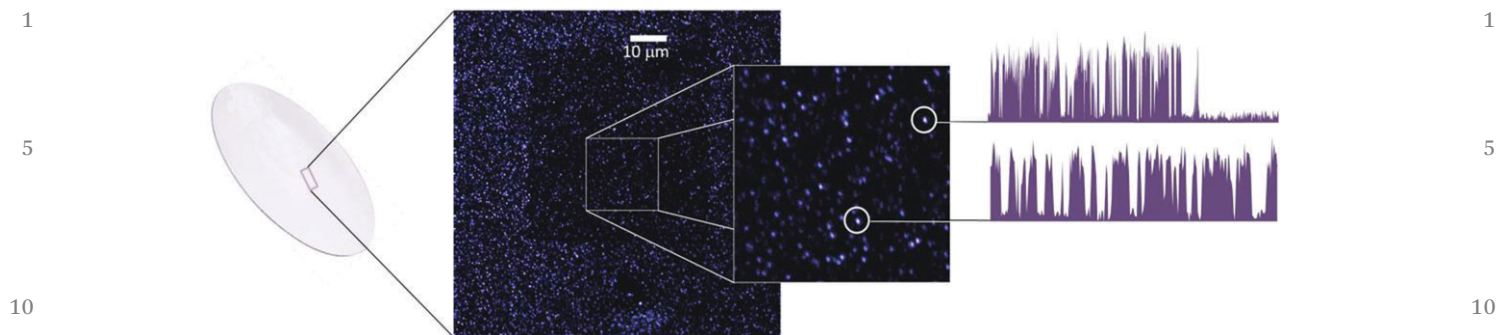Chem. Soc. Rev., 2014, **00**, 1—16 | 1

Fig. 1 From ensemble to single molecule detection. A dilute spread of single fluorophores on a cover glass shows zillions of single spots when viewed using a confocal fluorescence microscope. Zooming in further, each molecule shows up as a diffraction-limited spot. Tracing single molecules in time one observes abrupt photodissociation and discrete blinking due to triplet and other dark states. The different time traces from molecule to molecule readily show the stochastic response of the single molecule and the heterogeneity of the sample.
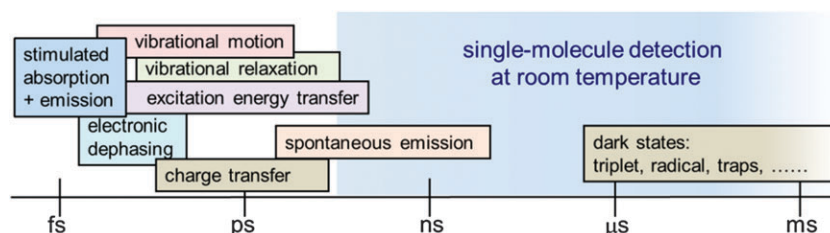

Fig. 2 Overview of the timescales of various molecular processes. The time resolution of standard single molecule experiments is indicated by the shaded blue area and does not reach the ultrafast timescale where most relevant electronic and vibrational dynamic processes take place.

the processes taking place in large organic molecules which are commonly studied in single molecule experiments. Unfortunately the spontaneous emission of a fluorescence photon is a relatively slow process typically occurring on a nanosecond timescale.[2–4] In contrast, electronic dephasing, excitation energy transfer, charge transfer, intramolecular vibrational energy relaxation and vibrational motions all occur on a femto- to picosecond timescale, much faster than the spontaneous fluorescence emission. As a result the ultrafast processes are out of reach for conventional fluorescence based single molecule detection and novel schemes are required to bring ultrafast spectroscopy to the realm of single molecules.

The study of femtosecond (fs) to picosecond (ps) molecular dynamics and energy transfer processes was, until recently, the exclusive domain of advanced ensemble pump–probe techniques, detecting large populations of molecules and yielding only average molecular response. The recurring principle of such pump probe experiments is the use of a short pulse to optically pump a set of molecules to a particular state, thus synchronizing a subset of the ensemble. Next, a second, delayed pulse probes the evolution of the created population. In most experiments, a fast, coherent process, such as excited state absorption is measured to follow the evolution of the system.

Bulk pump–probe techniques are limited to processes that can be optically synchronized; the implicit assumption underlying those experiments is that all molecules involved are identical, including having no or identical interaction with an environment (solvent, embedding crystal, carrier gas). A large

number of interesting (biological) processes do not meet this criterion, as these are, by definition, characterized by a high degree of static and dynamic disorder and are highly environment dependent.

At the same time, ultrafast processes play a crucial role in the functioning of both natural and synthetic molecular assemblies. Isomerization of the retinal in rhodopsins can happen on femtosecond timescales, starting the signalling pathway in vision; autofluorescent proteins undergo complex photocycles on timescales spanning several orders of magnitude; exciton transfer in conjugated polymers, holding the promise of molecular electronics, occurs at ultrafast timescales. Closely packed molecules interact *via* dipole–dipole coupling resulting in the transfer or even in the delocalization of the excited state energy over multiple chromophores, which is the basis of FRET, widely used as a labelling technique to measure proximity. The ultrafast energy transfer in light harvesting complexes is vital for collecting the sun's energy and converting it efficiently into the chemical energy needed to sustain life; remarkably in recent years intriguing coherences have been observed in the fs dynamics of such light harvesting complexes which are thought to play a role in the transfer efficiency.[11,12] All these types of assemblies, and biological systems in particular, feature a high degree of (conformational and electronic) disorder. It is therefore very relevant to investigate such heterogeneous molecular assemblies using a technique that allows us to differentiate the dynamics of individual quantum units (molecules, polymer chains, light harvesting complexes, proteins *etc.*), in interaction with their environment, at ultrafast timescales. The first step

towards achieving this goal is to detect such fast and coherent processes at the level of single quantum units.

The gap between the detection of ultrafast timescales and single quantum systems was first closed by Lienau and co-workers,[13] who studied quantum wells and dots, where at cryogenic temperatures the increased absorption cross-section allows standard pump probe methods to be used. A second set of interesting experiments, by Hell and co-workers,[14] used picosecond pulses at different wavelengths to suppress the fluorescence of individual molecules by stimulated emission depletion (STED) to increase spatial resolution in optical microscopy; indeed single molecule resolution towards 10 nm was achieved[15] and even the excited state absorption cross-section determined,[16] yet no time resolved information was reported.

A decade ago we started to explore fluorescence-detected pump–probe techniques to enable the detection of phenomena in single molecules taking place on femtosecond timescales and under ambient conditions. In 2004 we bridged the gap between "ultrafast" and "single molecule" detection by recording first ultrafast transients,[17,18] which was a first step towards addressing fs processes in molecular assemblies, to be studied on the nanoscale under ambient conditions.

In this review we present an overview of various ultrafast excitation schemes for the analysis of individual quantum systems. We show the various aspects of molecular dynamics that can be observed (electronic coherence decay, energy transfer) and induced (molecular qubit flipping, vibrational wavepacket interference) using these techniques. We further demonstrate that many photophysical parameters can be retrieved from ultrafast single-molecule data, e.g. pure electronic dephasing times, incoherent vibrational relaxation times, and vibrational energies. First we reconsider the potential of incoherent pump–probe (dump) single molecule spectroscopy, both single colour and two colour.[17,19] Next we move to more versatile coherent schemes, using broad band lasers and pulse shapers.[20] We demonstrate the detection and manipulation of vibrational wavepackets[21] and fs electronic coherence[22] in individual molecules in the excited state, all at room temperature. Finally we present two-colour phase control as an approach to address coherence in the energy transfer of multi-chromophoric photosynthetic light-harvesting complexes.[23]

2. Routes to ultrafast single molecule detection

Ultrafast fs spectroscopy on ensembles is generally realized in absorption contrast or through non-linear response. For example, in transient absorption spectroscopy one records the changes in the absorption spectrum as a function of the time delay of a probe to a fs pump pulse. Particularly powerful is 2-dimensional electron spectroscopy (2D-ES) which combines a $\chi^{(3)}$ 4-wave mixing scheme with a photon echo approach to determine the fs response over a broad range of frequencies, providing insight into both diagonal and off-diagonal coupling of electronic transitions.[11,12,24–26]

The very first single molecule detection (under cryogenic conditions) by the Moerner group was actually based on absorption.[1] Yet soon it was realized that the background-free fluorescence detection scheme devised by Orrit and Bernard was much more versatile.[2] Single molecule detection using counting fluorescence photons has dominated the field ever since.[3,4] For a single molecule with a fluorescence quantum yield close to unity and typical fluorescence lifetimes of 1–5 nanoseconds, typically 10^3 to 10^5 fluorescence photocounts are detected per second. As the photobleaching probability is typically 10^{-6} per photocycle for a fluorophore at room temperature, this results in observation times of a few seconds only. These relatively few and "slow" fluorescence photons are not easily compatible with detection of fs dynamics. Ideally, ultrafast single molecule detection would require a better detection scheme than one relying on fluorescence.

However, the absorption cross-section σ of a single molecule at room temperature is 10^6–10^8 times smaller than the area λ^2 of a diffraction-limited spot. Thus one faces a severe background problem in trying to distinguish the absorption of a single molecule against an incident laser beam. Yet recently interesting room-temperature experiments have been presented, by the Xie and Sandoghdar groups, showing the detection of individual fluorophores in direct absorption, using differential transmission techniques[27] and ultrasensitive balanced photodetectors[28,29] as well as by the Orrit group who exploited photothermal contrast to detect individual molecules and to determine the absorption cross-sections.[30] Unfortunately, for photothermal measurements high laser powers are required to locally heat the sample, which is not feasible for biomolecules, because these are very sensitive and easily disassemble under such conditions. Moreover, the signal-to-background of all these efforts does not deviate much from unity. In absorption measurements, this could be improved by close-by nanoparticles that enhance the absorption rate, yet, it is still unclear how the presence of such particles influences the molecular dynamics itself.

Raman scattering is an interesting alternative: Raman is fast (fs–ps) and free of the excitation background. Unfortunately the cross section for Raman is about 10^{12} times smaller than the cross-section for fluorescence, which renders detection of Raman scattering from a single molecule close to impossible. Using strong enhancement by metal nanoparticles (SERS, Surface Enhanced Raman Scattering), Raman spectra of single molecules have been detected.[31] Yet signals are weak and the molecule needs to be in very close proximity to a metal surface. Coherent Anti-stokes Raman Spectroscopy (CARS) provides ps resolution Raman spectra and has been realized with a sensitivity down to ∼10 molecules, by the Xie-group.[32] An interesting alternative to address single molecular vibrations, based on a three-photon fluorescence excitation scheme, was proposed by the Orrit group.[33]

Finally, detection of stimulated emission is the natural alternative to stimulated absorption measurements. Indeed the detection of a very small number of (non-florescent) molecules by stimulated emission has been shown.[34] The Hell

This journal is © The Royal Society of Chemistry 2014

Chem. Soc. Rev., 2014, 00, 1–16 | 3

group[16] used STED of fluorescence to measure the stimulated emission cross-section for the STED-transition of single molecules at room temperature. Yet the detection of stimulated emission of a single molecule at room temperature is still to be shown. Moreover, the stimulated emission signal is very sensitive to the wavelength, duration, and timing of the stimulation pulse. In combination with the complex pulse sequences needed to address ultrafast dynamics in molecular systems, this poses a big challenge at the single-molecule level.

Thus, despite progress on various alternatives, for single fluorescent molecules the best signal-to-noise and signal-to-background ratios are still achieved by recording the incoherent spontaneous fluorescence emission. All experiments presented in this review rely on fluorescence detection. This is done on an epi-confocal microscope. Single molecules are embedded in a thin (20–100 nm) polymer (PMMA, PVA) layer at a concentration of around 10^{-9} molar. Confocal microscopy consists of focusing a laser beam down to its diffraction limit and raster scanning either the sample or the beam to build up an image of intensity as a function of position. It relies on rejection of out-of-focus fluorescence by imaging the laser focus on a pinhole. In the case of the experiments described here, avalanche photodiodes with sufficiently small detection areas were used such that the detection area itself effectively functioned as a pinhole. While the pulse trains described in the various paragraphs are created in different fashions and with different lasers, the excitation–detection setup is identical. A high numerical aperture (1.3NA) objective is used to focus the light on the sample and collect the fluorescence emitted by the molecule. The fluorescence is separated from the excitation light by an appropriate dichroic mirror, passes suitable long-pass filters to reject residual laser light, and is finally detected using an avalanche photodiode. The sample scanning, delay-line positioning, pulse shapers, shutters *etc.* are all computer controlled.

The main challenge in ultrafast single molecule experiments is therefore to translate information about the ultrafast dynamics into changes in the probability for spontaneous emission, which is directly related to the excited-state population probability.

3. Incoherent single molecule pump–dump spectroscopy

In a typical fluorescence experiment, an electronic molecular transition S_0–S_1 is excited by irradiation with a light source, *e.g.* a short (femtosecond) laser pulse. If the fluorescence quantum yield (Φ_f) of the system is close to unity, the resulting photo-generated excited state will decay to vibrationally lower lying states *via* Intramolecular Vibrational Relaxation (IVR) on a picosecond timescale and, after some nanoseconds, the molecule will finally return to the electronic ground state by spontaneous emission of a photon. In an initial basic approximation we ignore coherent effects for laser pulses longer than the coherence time of the transition ($\sim$20–80 fs for large organic molecules at room temperature), such that population rates are sufficient to describe the dynamics. Then the competition between absorption and stimulated emission restricts the maximum population probability of photo-exciting a molecule to fifty percent, a limit situation referred to as saturation of the optical transition.

In the pump–dump experiments presented here an individual molecule is irradiated with two intense, short laser pulses whose mutual delay can be varied (Fig. 3A).[17,18] If saturation is achieved with the first laser pulse, adding a second identical pulse at the same time will not increase the chance that the molecule ends in the excited state. As a result, the fluorescent signal will not rise. The situation is different when the second pulse arrives after some delay. After the first pulse has passed, the molecule will have an equal probability to reside in the excited state or in the ground state. When the molecule was left in the excited state, it will have redistributed some of its energy
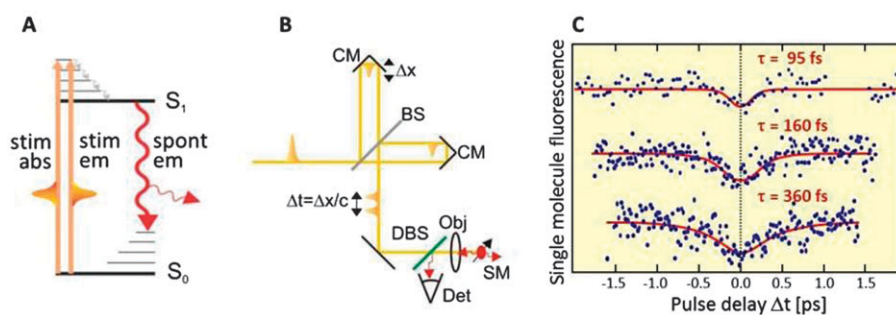

Fig. 3 (A) Scheme for fluorescence detection of an individual molecule in a single molecule pump–dump experiment. Two identical, intense and short laser pulses with variable time delay are used to excite the sample. After vibrational relaxation in the excited state S_1, the spontaneous fluorescence emitted to return back to the ground state S_0 is measured. (B) Scheme of the (single colour) pump–dump experimental setup. The short laser pulses are split on a beam-splitter (BS) and the length of one of the optical paths is varied by moving a corner mirror (CM). The pulse train passes a dichroic beam-splitter (DBS) and is focused using an oil immersion objective (Obj) on the sample containing single molecules (SM). The emitted fluorescence is collected by the same objective, reflected by the DBS and detected using an avalanche photodiode (APD). (C) Typical fluorescence response of 3 individual fluorophores as a function of the time delay between the pump and dump pulses. The dip around zero time delay reflects the timescale of excited state decay, due to intramolecular vibrational relaxation and electronic dephasing at the sub-100 fs timescale. Rather distinct decay times are observed for different, yet chemically identical, molecules in a polymer host. (Reproduced with permission from *J. Chem. Phys.*[18])

4 | *Chem. Soc. Rev.,* 2014, **00**, 1–16

This journal is © The Royal Society of Chemistry 2014

by the time the second pulse arrives. The molecule will be in a state from where it can no longer be stimulated back to the ground state by the second pulse and it will ultimately decay by emitting a fluorescence photon. If the molecule remained in the ground state after the first pulse passed, the second pulse will have a chance to excite the molecule, thus leading to an increase in the total fluorescence signal. Consequently, varying the time delay between the pulses will result in modulation of the fluorescence emission intensity, with a minimum in the detected signal for zero time delay. The rise time from the minimum to the plateau at long delays is a measure of the time that the molecule remains in the initial excited state. Molecules that redistribute their excited state energy quickly will result in more narrow minima. Using a three level model of the energy levels in the molecule and taking into account the length of the laser pulses it is relatively straightforward to fit the data and recover the energy redistribution time (τ_{er}). However, this model is too simplistic at timescales below 100 fs, for which coherence does play a role and the phase between the pulses needs to be taken into account, as we will see later.

Pump–dump measurements on single molecules are performed in an experimental setup schematically presented in Fig. 3B. Typically a mode-locked laser or (frequency doubled) optical parametric oscillator provides the visible laser pulses (here ∼280 fs, repetition rate 1 MHz) to irradiate the sample, while maintaining saturating peak powers. The laser pulses are split on a beam splitter and recombined on the same beam splitter after reflection on corner mirrors. One of the mirrors is placed on a translation stage allowing the delay between the pulses to be varied from −3 to +3 ps in a few seconds. The delay line is not phase-stabilized, such that the phase is averaged during the photon counting integration time. A shutter is placed in one of the branches such that one of the pulses can be temporally blocked and therefore the behaviour of the system followed under single pulse excitation. Further experimental details are presented elsewhere.[18] A typical fluorescence response of single molecules as a function of time delay is shown in Fig. 3C. The fluorescence decay around zero time delay is readily appreciated.

We have performed pump–dump experiments on various different individual fluorophores and studied the ultrafast pathways in these molecules. Fig. 4 shows representative data for two fluorophores typically employed in single molecule measurements: DiD (1,1′-dioctadecyl-3,3,3′,3′-tetra-methyl-indodicarbocyanine) and a perylene diimide (PDI) derivative (N,N′-dipropyl-1,6,7,12-tetrakis-(4′-tert-butylphenoxy)-3,4,9,10-perylenetetracarboxylic diimide). In both cases we can clearly identify the characteristic reduction in the fluorescence signal for zero time delay. The solid line shows the result of a fit to recover the redistribution times from the different dips. For each dip typically 10^4 photons have to be collected. This remarkably low number of photons made pump–dump experiments also possible on even relative photo-unstable dyes such as Cy5 and Atto590. Under similar experimental conditions these species stopped emitting after on average ∼3×10^4 photons were collected. Conversely, DiD and PDI are exceptionally photostable dyes (>10^5 photons collected before photo-reaction) which allow multiple pump–dump delay responses to be measured on the same molecule.

Interestingly, chemically identical molecules under the same conditions can have very different redistribution times. For the DiD molecules depicted in Fig. 4A we find τ_{er} values of 90, 160 and 350 fs. Measuring a large number of DiD molecules in the same matrix (poly(methylmethacrylate), PMMA) we recover a wide distribution of ultrafast decay times with an average time $\langle \tau_{er} \rangle$ = 230 fs, as indicated in Fig. 4C. Experiments on a large number of PDI dyes also embedded in a PMMA matrix result in a similarly broad range of energy redistribution times, however shifted to much shorter values ($\langle \tau_{er} \rangle$ = 95 fs). Here it should be noted that for times below 100 fs electronic dephasing will play a dominant role which limits the shortest times observable for PDI.

The fact that the average redistribution times are different for two chemically distinct fluorophores in the same matrix is a first indication that the process being probed is fluorophore specific. We have further investigated this issue by performing pump–dump experiments on the same dye (DiD) embedded in
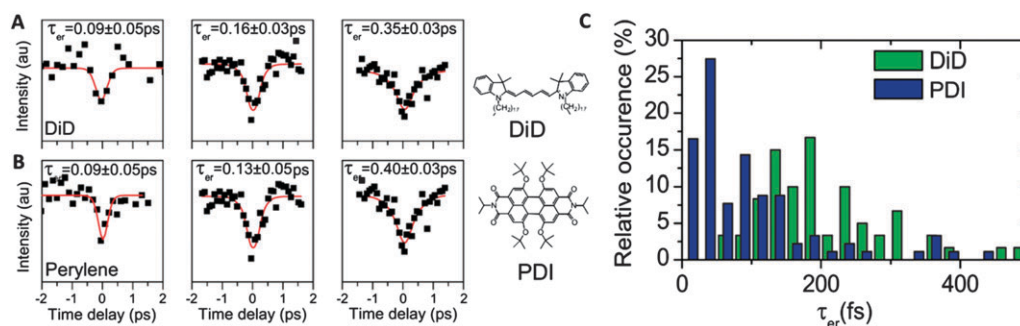
Fig. 4 Characteristic pump–dump response for two common fluorophores: (A) DiD in PMMA, (B) PDI in PMMA. For both types of fluorophores three different molecules are shown, exhibiting markedly different time scales. The solid lines indicate the result of fitting the dips with a model that takes the finite pulse width into account. The recovered redistribution times (τ_{er}) are indicated. The molecular structures of the fluorophores are also given in the figure. (C) Histogram of the energy redistribution times (τ_{er}) for two different fluorophores, DiD (λ_{exc} = 635 nm, excess of vibrational energy ∼850 cm^{-1}) and PDI (λ_{exc} = 575 nm, excess of vibrational energy ∼355 cm^{-1}). The average redistribution times ($\langle \tau_{er} \rangle$) are 230 fs and 95 fs for DiD and PDI, respectively. (Reproduced with permission from J. Chem. Phys.[18])

This journal is © The Royal Society of Chemistry 2014

Chem. Soc. Rev., 2014, 00, 1–16 | 5

two different polymer matrices (PMMA and Zeonex). A very minor effect of the surrounding matrix on τ_{er} has been encountered, the average redistribution times measured for both samples under equivalent excitation conditions taking similar values ($\langle\tau_{er}\rangle$ = 230 fs for PMMA and $\langle\tau_{er}\rangle$ = 180 fs for Zeonex). Therefore, we conclude that the pump–dump experiments mainly report on an *intra*molecular process. Indeed, solvent-independent (sub-)picosecond relaxation times in optically excited fluorophores are commonly assigned to intramolecular redistribution of the excited state energy over different vibrational states just after excitation: intramolecular vibrational energy relaxation (IVR).[35] When a molecule is brought into an electronically excited state, IVR ensures a quick redistribution of the vibrational energy of the system over different vibrational modes, while the transfer of its excess of vibrational energy to the environment takes place on a longer (picoseconds) timescale. Noticeably, the initial redistribution of the energy already leaves the molecule in a state from where it can no longer be stimulated back to the ground state. The time measured therefore reports on such an initial IVR process, which results from the coupling between the electronic and vibrational modes of the molecule. A strong coupling will result in a fast redistribution of the energy and thus narrow minimum. Wider minima on the other hand are an indication of a reduced coupling between optically active and inactive modes, resulting in the molecule remaining longer in the initially excited state. The intramolecular coupling determining the IVR dynamics actually depends on several variables, such as the nature of the initial Franck–Condon state prepared by optical excitation, the density of vibrational states it can couple with and the coupling matrix elements between those states.[36] Together with the influence of electronic dephasing, the τ_{er} differences encountered for distinct fluorophores in our single molecule experiments are hard to rationalize, which complicates direct comparison with IVR times reported in bulk for similar molecules.[37]

The broad distribution of times indicates that in a polymer host at room temperature chemically identical molecules do display large variations in the ultrafast redistribution of their excited state energy. Single molecule experiments have shown

already large variations of several spectroscopic parameters for "identical" molecules. For instance the triplet state and singlet excited state lifetime and fluorescence spectra have been shown to vary from molecule to molecule.[7–9] Here, however we find that these variations even extend to *intra*molecular processes on femtosecond timescale. These variations are indicative for the different conformational states of the individual molecules that are induced by the nano-environment. Different conformations result in variations in the coupling between the electronic and vibrational modes, an effect that was observed before in steady state single molecule fluorescence emission spectra.[38] These previous studies reported on the coupling between the electronic and ground state vibronic modes, the single molecule pump–dump data now report on the processes taking place in the electronically excited states.

The single colour pump–dump scheme can be extended to a two colour pump–dump scheme to address specific initial and final states. The pump pulse is followed by a red shifted saturating dump pulse which depletes the excited state, in direct competition with the generated fluorescence (Fig. 5A). This scheme is identical to stimulated emission depletion (STED) used for STED microscopy.[14] Fig. 5B shows the fluorescence reduction for DiD molecules with 250 fs pump pulse at 580 nm and dump (STED) pulse at 750 nm. Indeed fluorescence can be reduced; however the efficiency depends on the spectral–temporal overlap of the dump pulse with the involved vibrational states. Only for stretched pulses (>4 ps) an appreciable reduction in fluorescence can be achieved due to long-lived vibrational states in the electronic ground state. As a result the decay time reflects the pulse length of the dump pulse, while the recovery time tends towards the fluorescence lifetime. Thus effective stimulated emission depletion comes with loss of information on sub-ps dynamics. The time-bandwidth content of the dump pulse requires further fine-tuning.

An alternative pump–probe scheme can be contemplated (Fig. 5C), in which the ground state vibration is populated directly by an IR pump pulse, followed by a visible probe pulse driving the molecule to the electronic excited state for subsequent fluorescence read-out. A similar scheme was also
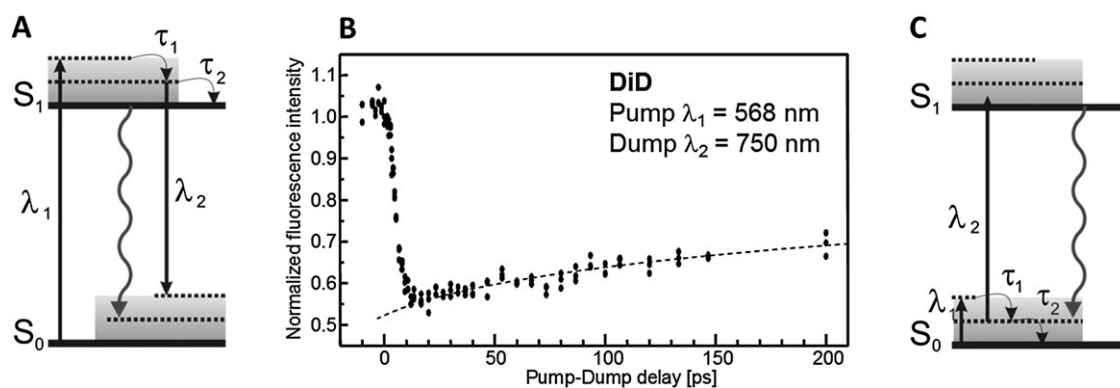
Fig. 5 (A) Two colour pump–dump scheme. (B) Two colour pump–dump spectroscopy on DiD molecules. Pump pulse, 250 fs, at 568 nm; dump pulse stretched to 5 ps, at 750 nm. (C) IR-visible pump–probe scheme.

proposed by Orrit and colleagues.[33] So far this scheme has not yet been realized for single molecules, as the transitions need to be saturated and direct single and two photon excitations of the molecule result in a fluorescence background which complicates detection of the effect of the IR pump.

Despite the results shown the incoherent pump–dump scheme has a few severe drawbacks. First, for both pulses to interact with a single molecule the transitions need to be saturated. Obviously single molecule excitation at saturation power density results in fast photobleaching. Even for photo-stable fluorophores (10^6 photo cycles) and a reduced repetition rate (1 MHz) the typical observation time is only seconds. Second, the lack of a phase relation between pump and dump pulses prevents disentangling the role of coherence and dephasing effects in the recorded time traces. Clearly a coherent excitation scheme operating in the non-saturating regime is largely preferred, which is the topic of the next sections.

4. Control of single molecule electronic coherence

The next step in fs excitation of single molecules is to gain control over both the time delay and the relative phase between both pulses. An interesting extra dimension then opens up in the experiments. The experiment can now be described as the first pulse creating a coherent superposition state in the molecule, and the second pulse probing the phase memory in that coherent superposition created by the first pulse. After interaction of the molecule with such pulse sequences, the excited state population probability, and with it the incoherent spontaneous emission, becomes a function of both inter-pulse delay time and phase difference. Notably, the time-phase dependence of the fluorescence can be related to molecular properties influencing excited state dynamics, for example through pure electronic dephasing and incoherent vibrational

relaxation. Equally important, the effect of phase control is detected through interference between the molecular polarization induced by the field of the first pulse, and the field of the second pulse. In this picture, the concept of saturation does not hold anymore and meaningful experiments can already be done at low excitation powers.

Fig. 6 depicts the basic notion of the coherent approach for a two-level system. A single molecule is resonantly excited into the purely electronic transition between the electronic ground ($|1\rangle$) and excited states ($|2\rangle$) by femtosecond double-pulse sequences. At variance with previous pump–dump schemes, now the pulses are phase-locked. The excitation induces stimulated absorption and emission processes and prepares the two-level system in a certain state, which is best visualized by a Bloch vector on a Bloch sphere of unity radius (Fig. 6A). The Bloch vector pointing to the poles represents an eigen-state of the two-level system, while any other position indicates a coherent superposition between levels $|1\rangle$ and $|2\rangle$. Interaction with the first pulse generally creates a coherent superposition state corresponding to a rotation of the Bloch vector away from its initial ground-state position. First, we consider the simplest case of the molecule completely isolated, *i.e.* free of dephasing (Fig. 6B, left). Fixing the phase difference $\Delta\phi$ at 0 rad, the second pulse rotates the Bloch vector further about the same axis as the first pulse (Fig. 6B, top left sphere) and its final position is independent of the delay time Δt, as interaction with the light field is the only process changing the state of the Bloch vector. Second we consider the molecule embedded in a disordered environment at room temperature (Fig. 6B, right); *i.e.* dephasing by interactions with the matrix rapidly erases the phase memory between the ground- and excited-state wavefunctions (with the electronic dephasing time T_2^*). As a result the magnitude of the Bloch vector reduces below unity and decreases with time. Now the final position of the Bloch vector tip after the pulse sequence changes and becomes a function of Δt, with decreasing excited state population (Fig. 6B, top right
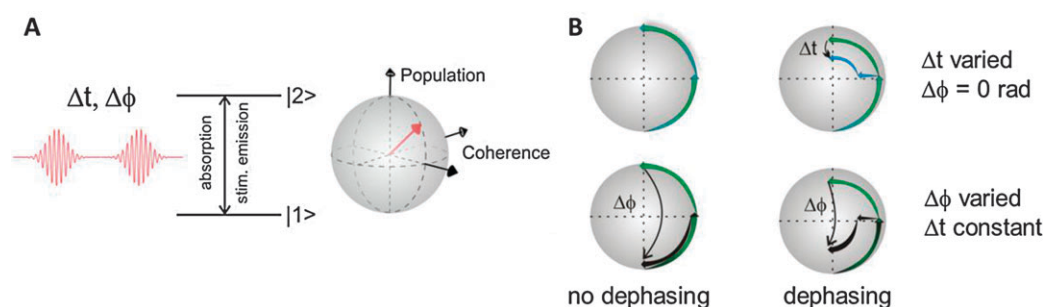

Fig. 6 Coherent excitation of a two level system. (A) A sequence of phase-locked ultrashort pulses resonantly drives a single molecule between the ground ($|1\rangle$) and lowest excited levels ($|2\rangle$). The state of this two-level system is visualized using the Bloch vector (red arrow) on the Bloch sphere, where the poles correspond to the eigenstates ('south': $|1\rangle$, 'north': $|2\rangle$) and any other point indicates a coherent superposition between ground- and excited-state electronic wavefunctions. (B) Influence of varying the delay time Δt and relative phase $\Delta\phi$ on the trajectories of the tip of the Bloch vector. Without electronic dephasing a change of Δt at constant $\Delta\phi$ does not affect the trajectory (top left sphere). In contrast, in the presence of dephasing the magnitude of the Bloch vector continuously decreases resulting in a measurable change in the exited-state population for increasing Δt (top right). The introduction of a phase change $\Delta\phi$ (at constant Δt) allows to manipulate the coherent superposition state by altering the rotation direction of the Bloch vector (bottom). The fidelity of preparation of coherent superposition states is reduced with dephasing (right) as compared to the situation without dephasing (left). (Reproduced with permission from *Nat. Phys.*[22])

This journal is © The Royal Society of Chemistry 2014

Chem. Soc. Rev., 2014, **00**, 1–16 | 7

sphere, green and blue arrows). Recording the decay of the fluorescence with Δt provides information about the residual coherent superposition state of the molecule. More specifically the degree of (de)coherence can be probed by exploiting the relative phase $\Delta\phi$ between the electric fields of the laser pulses, because $\Delta\phi$ determines the rotation direction of the Bloch vector induced by the second pulse. A π phase shift fully inverts the rotation direction and moves the Bloch vector back towards its ground-state position (Fig. 6B, bottom, green arrows: $\Delta\phi = 0$, black arrows: $\Delta\phi = \pi$). The change of $\Delta\phi$ therefore allows manipulating the motion of the Bloch vector at a discrete time during loss of phase memory, giving direct insight into the dephasing dynamics of single molecules.

Pulse pair generation by a simple delay line is not sufficient to independently control both time delay and phase difference between pulse pairs; for this, one needs a pulse shaper. An acousto-optic programmable dispersive filter (AOPDF, Dazzler, Fastlite) is a versatile pulse shaper, exploiting acoustic waves travelling in a birefringent acousto-optic crystal to achieve amplitude and phase shaping of an incident fs-pulse. Unfortunately an AOPDF only allows limited bandwidth and low pulse repetition rates. Here we used such an AOPDF to shape the output of an optical parametric oscillator with 18–21 nm FWHM spectral bandwidth, and compress the pulses to the transform-limit of 70–75 fs (FWHM). Moreover a pulse picker reduced the 76 MHz repetition rate to effectively 500 kHz (bunches of pulses with a repetition rate of 25 kHz, repetition rate within bunches: 4 MHz) to match the input of the AOPDF. With the operation conditions for an AOPDF met, the shaper was used to control both delay time Δt and phase difference $\Delta\phi$ between the electric fields of the output pulses. The output of the AOPDF was spatially filtered in a lens–pinhole-lens combination, and directed into a confocal microscope.

As a test case to influence single molecule electronic coherences, we excited single TDI (terrylenediimide) molecules in a PMMA film with the phase-locked double-pulse sequences.[22] We used a central wavelength of 630 nm to excite into the purely electronic transition of individual TDIs. Examples of quantum coherence in single molecules with several fluorescence traces as a function of Δt and $\Delta\phi$ are shown in Fig. 7. Fig. 7A and B depict time delay traces with $\Delta\phi$ fixed at 0 rad (black curves) with the time-averaged excitation intensity being kept constant during the acquisition of each trace. The emission signals in Fig. 7A and B feature pronounced variations of up to a factor of 2 with decay and recovery times, respectively, of several tens of fs, which reflect the decay of coherences of the TDI molecule with a time constant of about 50 fs. For $\Delta t >$ 300 fs, the emission remains constant. The change from decaying to rising trace (Fig. 7A and B) is due to stronger interaction between the laser field and the molecular transition dipole moment, i.e. an increased Rabi-frequency. Numerical simulations (red lines) based on the optical Bloch equations for a 2-level system yield a Rabi-frequency of 0.01 fs^{-1} and 0.06 fs^{-1} in A and B, respectively, consistent with the higher number of detected photons in B for long delay times. Note that spontaneous emission and non-radiative transitions to the ground
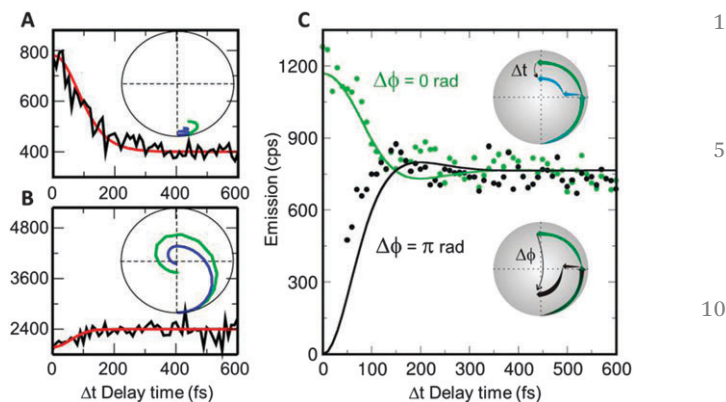

Fig. 7 Controlling the coherent superposition state of a single molecule (TDI in a PMMA film). (A and B) Black lines: fluorescence as a function of the delay time Δt between the pulses for two single molecules under low and high emission rate conditions, respectively ($\Delta\phi = 0$ rad; cps: counts per second). Red lines: numerical simulations based on the optical Bloch equations for a 2-level system with Rabi-frequency 0.01 fs^{-1} in A and 0.06 fs^{-1} in B, respectively. Inset: development of the tip of the Bloch vector in time for delays of $\Delta t = 0$ fs (green) and $\Delta t = 400$ fs (blue), respectively. For the highest Rabi-frequency (B) a full Rabi-oscillation is observed. (C) Delay traces with $\Delta\phi = 0$ rad (green dots) and $\Delta\phi = \pi$ rad (black dots) measured on the same molecule. The solid curves represent numerical simulations with a Rabi-frequency of 0.03 fs^{-1}. Note that for both phase settings the excitation intensity was always constant during acquisition of the traces. (Reproduced with permission from Nat. Phys.[22])

state have been neglected in the fit, because these processes do not contribute within the first 600 fs after excitation. The insets visualise the time-dependent trajectories of the tip of the Bloch vector on the Bloch sphere. The trajectories are displayed for the corresponding traces in A and B for delays of $\Delta t = 0$ fs (green) and $\Delta t = 400$ fs (blue). In Fig. 7A the Rabi-frequency is rather small (only absorption takes place) and the excited state population probability decreases with Δt due to dephasing, with a correspondingly shorter Bloch vector. The nutation angle of the Bloch vector increases with rising Rabi-frequencies and also stimulated emission during interaction with the laser pulses becomes important. In Fig. 7B a full Rabi-oscillation is observed (nutation angle 2π), while again the magnitude of the Bloch vector decays with time due to pure electronic dephasing; effectively a rising emission signal as a function of Δt is observed.

It is fascinating to be able to monitor the evolution of the coherent superposition state of a single molecule at room temperature. For delays shorter than the electronic dephasing time T_2^* one should be able to manipulate the coherent state by variation of $\Delta\phi$ and subsequent rotation of the Bloch vector. In particular, a π phase difference exactly reverses the rotation direction of the Bloch vector. An example of delay traces with $\Delta\phi$ flipped from 0 to π is shown in Fig. 7C, with the time-averaged excitation intensity being kept constant during the acquisition of each trace. The green dots for $\Delta\phi = 0$ feature the decay of several tens of femtoseconds, while for $\Delta t > 300$ fs, the emission remains again constant. A fit (green line) gives $T_2^* = 60$ fs and a Rabi frequency of 0.03 fs^{-1}.[23] The black dots in Fig. 7C show a time delay measurement on the same molecule

8 | Chem. Soc. Rev., 2014, 00, 1–16

This journal is © The Royal Society of Chemistry 2014

with the pulses out-of-phase ($\Delta\phi = \pi$). Clearly the coherence results in destructive interference and reduced probability to reach the excited state. It should be noted that the time-averaged excitation intensity was kept constant for all time delay; thus the fluorescence reduction reflects purely the molecular coherence. These data demonstrate convincingly the potential to manipulate the Bloch vector of single molecules at room temperature despite femtosecond dephasing times; for $\Delta t < T_2^*$, the Bloch vector can be rotated to any arbitrary position and any coherent superposition state, by an appropriate choice of Δt and $\Delta\phi$.

Comparing the coherent time delay response in Fig. 7 to the incoherent pump–dump response in Fig. 4,[18] it becomes clear that the incoherent experiments contain a phase averaged contribution of the electronic coherence at time scales below 100 fs, while for longer times incoherent vibrational relaxation comes into play. In fact, interplay between electronic dephasing and vibrational relaxation was also observed in the coherent time delay experiments, showing distinctly different time constants which allows disentangling both effects; for details see ref. 20.

5. Single molecule vibrational wavepacket interference

Having established basic phase control of individual molecules, now let's extend the method to excitation by broadband pulses, covering all vibrational sidebands of the electronic transition. With this, one enters the realm of coherent control: the targeted steering of a quantum system through phase shaped excitation pulses into one state from a multitude of accessible ones. Obviously we aim to maintain the potential of single molecule detection. The coherent control of dynamic processes in molecular ensembles has been implemented in very sophisticated experiments in the last two decades.[39] Using cleverly tailored ultrashort femtosecond pulses, steering of reaction pathways, optimizing energy conversion[40–42] and control of spatial confinement of optical fields[43,44] has been shown. Particularly for complex systems such as large (bio)-molecules with many nuclear and electronic degrees of freedom, for which *ab initio* quantum mechanical calculations fail, the elegant approach of genetic self-learning algorithms has led to the coherent control of a wide variety of photo-induced processes.[41,42] The resulting optimized pulse shape reflects the dynamics of the underlying processes. The closed-loop experiments require a large number of iterations; as a result such approaches are out of reach for fluorescent single molecules, which bleach on a time scale of seconds and provide only a limited number of photocounts. Fortunately optimal control theory and experiments on large molecules have demonstrated that complex pulse shapes can often be simplified to physically more intuitive shapes based on trains of pulses with controlled width, delay and phase relations. Therefore we address single molecules with pairs of broad-band pulses, again varying time delay between the envelop Δt and relative carrier phase difference $\Delta\phi$.[20] We demonstrate the observation of vibrational wavepacket interference and phase control of the wavepacket for an individual fluorophore at room temperature.[21]

As a molecule of study we use an even higher rylene homologue than the TDI in the previous section: dinaphtho-quaterrylenebis(dicarbox-imide), in short DN-QDI.[45] DN-QDI is a photostable fluorophore with high quantum efficiency. With its 4 naphthalene units the absorption spectrum is shifted to the near-infrared with a maximum at 700 nm (in toluene
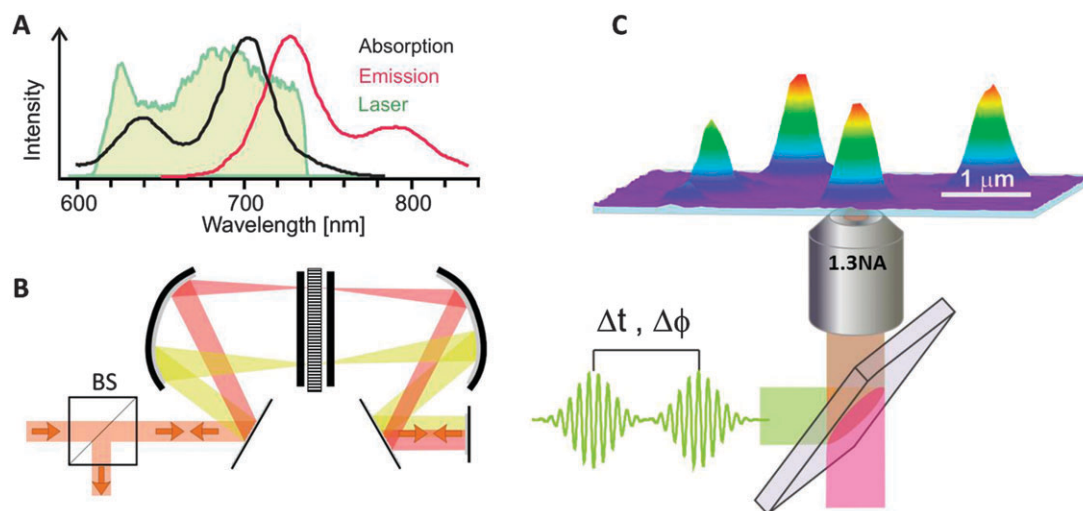

Fig. 8   (A) Absorption and emission spectra of the fluorophore (DN-QDI, dinaphto-quaterrylenebis(dicarboximide)[42]) and the broad-band excitation of the laser used. (B) 4f pulse shaper based on a spatial light modulator (SLM), operating in double-pass by passing the beam through a beam splitter (BS) and putting a mirror at the output of the shaper. (C) Single fluorescent molecules are excited and detected in an epi-confocal microscope. Each individual molecule is excited with shaped sequences of pulses, with an inter-pulse time delay Δt and phase shift $\Delta\phi$ as controlled by the 4f shaper. (Reproduced with permission from *Nature*,[21] *Opt. Express*.[47])

solution), see Fig. 8A. DN-QDI exhibits a prominent vibrational progression, at around 1350 cm^{-1}.

The coherent broad band excitation is provided by the output of a 85 MHz repetition rate mode-locked Octavius Titanium:Sapphire-laser (Octavius-85M, Menlo Systems, Thorlabs). The Octavius spectrum stretches from ∼550 nm wavelength to deep into the infrared, spanning an "octave" in frequency, providing a 7 fs pulse when Fourier limited. Here we selected a spectral bandwidth of 120 nm (15 fs) around the central wavelength of 676 nm (green band in Fig. 8A), thus covering nearly the entire DN-QDI absorption spectrum, and interacting with a manifold of vibrational levels in the electronically excited state. We employed a 4f-pulse shaper based on a Spatial Light Modulator (SLM) for dispersion control and pulse shaping (Fig. 8B). The 4f-pulse shaper was in-house adapted from a commercial shaper (MIIPS-box, Biophotonics Solutions Inc.).[46] Pulse calibration was performed using Multiphoton Intrapulse Interference PhaseScan (MIIPS) with the second harmonic spectrum being detected in the sample plane. The shaper is designed in a double-pass configuration[47] with a mirror at the end of the beam path reflecting the light back for a second pass through the shaper (Fig. 8B). This double-pass configuration minimises spatio-temporal coupling and allows larger phase distortions to be compensated.[47] In all experiments pulses were first compressed to their transform limit of 15 fs (about ±0.1 rad residual spectral phase variation) in the sample plane, using a MIIPS control loop.[46] Finally, as in the previous section, single molecules are excited and detected using a confocal microscope with a high 1.3NA objective and single photon counting avalanche photodiodes (Fig. 8C).

Fig. 9 shows a typical image of a set of individual DN-QDI molecules. The molecules are excited by a delayed pulse pair with an increasing inter-pulse time delay of Δt = 0, 21 and 42 fs, as controlled by the 4f shaper. The excitation power of the pulse pair is kept constant while the carrier phase difference Δϕ between each pulse pair is set to zero. The set of images gives a representative picture of the signal levels and dynamics
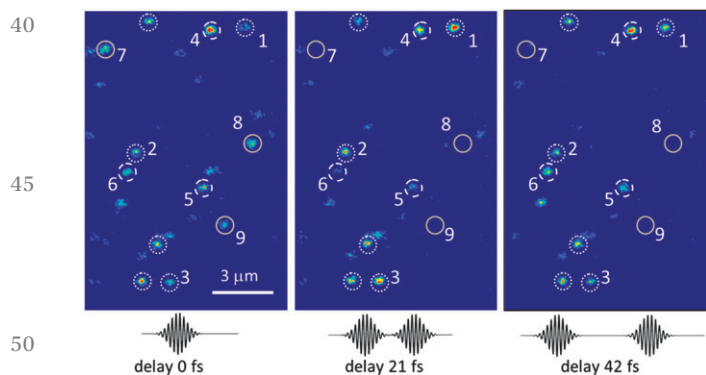

Fig. 9 Fluorescence images of a set of individual DN-QDI molecules excited by a delayed fs pulse pair with 0, 21 and 42 fs delay, respectively. Note the different response amongst molecules: molecules 1, 2 and 3 show dim−bright−dim, while molecules 4, 5 and 6 show bright−dim−bright. Molecules 7, 8, 9 bleached after the first image. (Reproduced with permission from RSC *Faraday Discuss.*[21])

observed in fs single molecule excitation. Diffraction limited spots (∼300 nm FWHM) are observed with different fluorescence intensity, sometimes noisy due to the limited signal/noise ratio (about 10) when detecting single molecules. Upon close inspection of the different panels (0−21−42 fs) one observes molecules #1, 2 and 3 to change from dim to bright to dim. In contrast molecules #4, 5 and 6 rather change from bright to dim to bright. Similar other cases can be discerned. Finally certain molecules, such as #7, 8 and 9 show up in the first panel, but have bleached and disappeared in subsequent panels. The differences from molecule to molecule clearly reflect the heterogeneity at room temperature; each molecule has a slightly different conformation and experiences a locally distinct polymer environment. The heterogeneity affects the molecular dynamics, also on a fs time scale.

Fig. 10A shows the fs time delay (Δt) response of a selected individual molecule for both in-phase (Δϕ = 0) and in-antiphase (Δϕ = π) excitation pulses. The relative fluorescence is normalized to the fluorescence at long time delay. The single molecule response shows a strong oscillation of ±10% of the average signal. The oscillations are caused by wave-packet interference: constructive or destructive interference of the excited state wave packets generated by the delayed pulse pair. The wavepacket interference is nicely confirmed by the inverse phase control for (Δϕ = 0) and (Δϕ = π) excitation. Here it should be noted again that the excitation power has been kept constant in all cases. The oscillations persist up to ∼100 fs with a period of typically 30–40 fs. Fourier analysis shows a dominant frequency at around 1000 cm^{-1} (33 THz). Investigating more individual molecules we find distinct oscillations, with a distribution of characteristic wavepacket frequencies and markedly different oscillation phases from molecule to molecule.[21] The ultrafast response of each molecule is determined by the characteristics of its excited state potential energy surface; *i.e.* in a first approximation by the spectral positions, widths and strengths of the vibrational lines of the absorption spectrum.

The induction of wavepacket interference through excitation by a pulse pair, and the ability to control this interference through the time-phase structure of the excitation pulses, as shown in Fig. 10A, opens the route to full coherent control: optimisation of the excitation into a final state by a pulse sequence with tailored time-phase structure. To explore phase space we designed a series of multiple pulses (four) and systematically varied both their mutual delay time Δt and phase difference Δϕ. Fig. 10B shows the fluorescence in time-phase space for a selected single molecule. Clear fluorescence maxima and minima are observed at certain time-phase combinations. A ∼50% maximum at Δt = 20 fs with Δϕ = 0.7π and a ∼50% minimum at Δt = 20 fs with Δϕ = 1.7π again confirm the phase control, when switching to the anti-phase. The ratio between the maximal and minimal response is ∼3: a fairly high ratio for coherent control experiments, especially at room temperature. The π-shifted maxima and minima follow time-phase lines with a slope of about 23 fs/π. The wave-packet phase evolution can be traced by the optical field, giving insight into the wave-packet group velocity of the chosen molecule. Moreover tracing
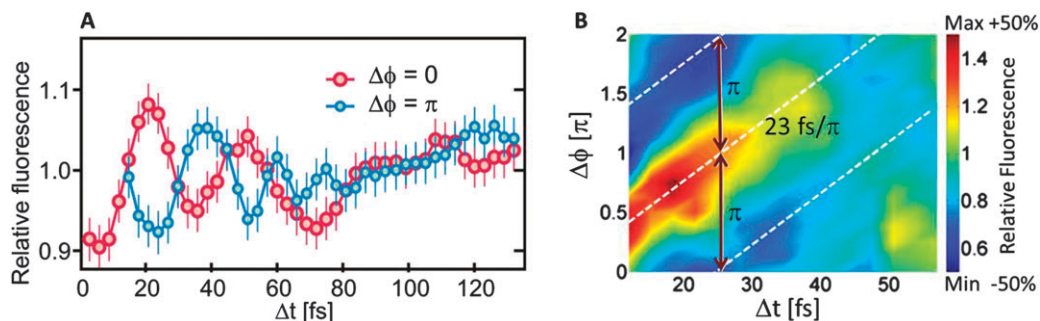
Fig. 10 Time-phase control of single-molecule wave packets. (A) Single-molecule fluorescence intensity as a function of the time delay between two in-phase ($\Delta\phi = 0$) and in-antiphase ($\Delta\phi = \pi$) excitation pulses. The excitation intensity was constant for all (Δt, $\Delta\phi$) combinations except for the (excluded) points near zero delay with $\Delta\phi = \pi$. While the main frequency component is around 30 THz (1000 cm^{-1}), the influence of other frequency components is seen. (B) Time-phase fluorescence excitation maps with a four-pulse sequence, with a Δt time delay and a $\Delta\phi$ phase shift between each consecutive pulse in the sequence. The maximum/minimum fluorescence ratio of $\sim$3 is achievable through optimization of coherent excitation. The maximum develops as 23 fs/π in the time-phase space. (Reproduced with permission from *Nature*.[21])

the time-phase line one can deduce a decoherence time of 30–40 fs.

6. Two colour phase control of energy transfer in light harvesting complexes

With the basic toolbox for coherent fs single molecule spectroscopy set, we now turn to an important application: ultrafast energy transfer in photosynthetic complexes. In recent years energy transfer in these systems is receiving great attention because of the observation of coherences in 2D-spectroscopy both at cryogenic and at room temperatures, by the Fleming, Scholes and Engel groups.[11,12,25] Particularly the discovery of long-lived electronic coherences, up to 200–300 fs, in various photosynthetic complexes (FMO – Fenna–Matthews–Olson; phycobiliproteins from marine cryptophyte algae; LH2 light harvesting 2 complex) has generated strong efforts, both in experiment and theory, to understand their origin and their potential role in biological function. Much of the controversy surrounding these observations stems from the question whether the coherences observed are purely induced by the excitation schemes, or whether they have biological function; and whether the nature of the observed coherence is electronic or vibrational. Moreover, the occurrence of coherences in pigment–protein complexes under physiological conditions challenges the common notion that interactions with the local environment universally lead to decoherence; possibly the protein scaffolds protect electronic coherences.

So far experimental approaches have concentrated on 2D-electronic-spectroscopy on ensembles of pigment–protein complexes at various temperatures[11,12,24] and on synthetic multichromophoric model systems.[26] Unfortunately therefore, any observed coherence is a spatial and temporal average over an inhomogeneous distribution and therefore hard to relate to a particular functionality in complex natural systems. Consequently the work presented here on coherent ultrafast detection of individual complexes is vital to unravel the role of coherence in the efficiency of natural photosynthetic complexes.[23]

We address energy transfer in the light-harvesting 2 (LH2) complex of purple photosynthetic bacteria *Rhodopseudomonas acidophila*. LH2 is a ring shaped pigment–protein complex composed of 9 identical subunits, each containing an α- and a β-helix which coordinate 1 carotenoid and 3 bacterioChlorophyll a (bChl a) pigments. The specific binding of the subunits results in the formation of two bChl pigment rings comprising 9 and 18 bChls, respectively. The 9 weakly interacting bChls absorb at ∼800 nm (B800 ring), and the 18 strongly excitonically interacting bChls absorb at 850–860 nm (B850 ring), Fig. 11A. Light energy absorbed by the carotenoids or the B800 ring is transferred in about 1 ps to the B850 ring from which the emission occurs with a fluorescence quantum yield of about 10% at room temperature. Single LH2 has been studied extensively, both at cryogenic and room temperatures.[48–50] The spectroscopic features, including the excitonic coupling in the B850 band, are well documented. The B800–B850 energy transfer is governed by an electronic coupling with intermediate strength, which raises interest in the potential role of quantum coherence in the transfer. For instance, recently a highly optimized 2D spectroscopy of LH2 in solution was performed by the Engel group, searching for the characteristics of the transfer mechanism in LH2.[51]

To address B800–B850 energy transfer in single LH2 complexes we designed a specific two-colour experiment.[23] Laser and 4f-shaper were identical to those described in previous Section 5, but a more red-shifted spectral band was selected. The broad-band 15 fs pulse (grey spectrum in Fig. 11A) was phase-shaped into two time-delayed transform limited pulses with different carrier frequencies that overlap with the B800 and B850 absorptions of LH2, respectively (Fig. 11B). This was achieved by pure phase shaping: a linear phase ramp was selectively applied to the appropriate spectral band in a pulse shaper (green line in Fig. 11A). The slope and off-set give full control over both the delay time, Δt, and the relative carrier envelope phase, $\Delta\phi$, between both pulses. We detected the fluorescence signal, that is, the total population probability of the lowest-energy and emitting B850 exciton state after interaction with both pulses.
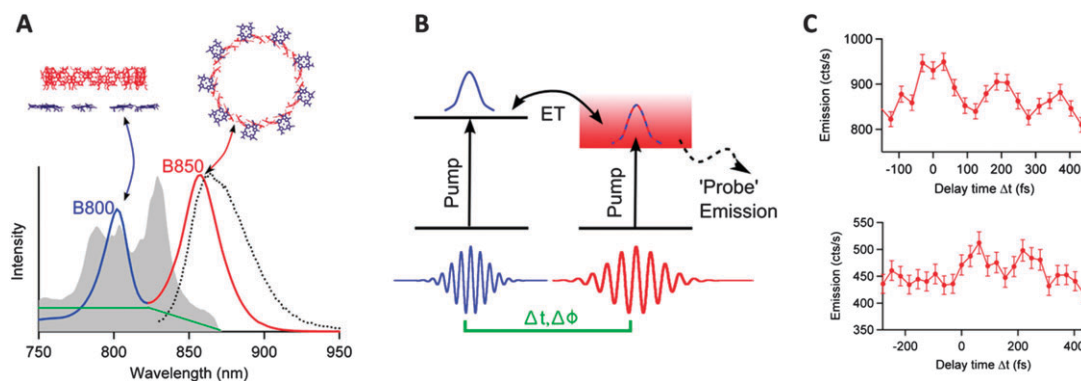
This journal is © The Royal Society of Chemistry 2014

Chem. Soc. Rev., 2014, **00**, 1–16 | **11**

Fig. 11 Two colour fs phase control of individual light harvesting 2 (LH2) complexes at room temperature. (A) The LH2 complex of the purple bacterium *Rps*. acidophila consists of two rings of Bchl-a pigments: the B800 ring with 9 fluorophores (blue) and the B850 ring with 18 fluorophores (red), with the characteristic near-infrared absorption bands at 800 and 850 nm, respectively. The exciting laser spectrum is depicted in grey. The green line represents the spectral phase function applied by the 4f-pulse shaper to generate the pulse pair. (B) Concept of the experiment: single LH2 complexes are excited by a two-colour pulse pair with Δt and $\Delta \phi$ generated by applying the spectral phase function. The first (blue) pulse creates an excitation in the B800 band. After energy transfer (ET) to the B850 band, the second (red) time-delayed pulse, resonant with the B850 band, modulates the population transfer to the B850 excited states by quantum interference. The resulting probability is probed by detecting the spontaneous emission from a single complex. (C) Ultrafast fs single molecule data taken on two different individual LH2 complexes. The traces show oscillatory fluorescence intensity variations in dependence of the time delay between the two excitation pulses of different colours. (Reproduced with permission, *Science*.[23])

Fig. 11C shows two typical two-colour time delay traces of individual LH2 complexes for phase difference $\Delta \phi$ between the two excitation pulses equal to zero. Both complexes exhibit oscillations up to at least 400 fs, with periods of around 200 fs and a contrast of about 15%. The oscillations are attributed to quantum interference between two excitation pathways that populate the same target state, the emitting lowest-energy B850 level. Investigating more LH2 complexes, persistent coherence was observed in many cases, while the interference oscillations occurred over a wide distribution of periods between 140 and 400 fs with a maximum near 200 fs.[23] This broad spread in T implies that each complex features a distinct transfer pathway characterized by its period T. The distribution of T is consistent with an average electronic coupling of $J \approx 50$ cm^{-1} between B800 and high-energy B850 states, indicating that optically dark high-energy B850 exciton states are involved in these first transfer steps.[23]

It is intriguing to find that the coherences in LH2 persist almost 10 times longer than the coherences of an isolated fluorophore in a solid state polymer environment (see Fig. 7 and 10). Both the protein scaffold and the relatively strong electronic coupling play a role in protecting the coherence. The interplay between the persistent coherence and energy dissipation by interactions with the surrounding bath directs the excitation energy rapidly toward the lowest-energy B850 target levels, from which further transfer to adjacent complexes occurs. The quantum coherences survive long enough to allow averaging over local inhomogeneities of the excited-state energy landscape and thus to avoid trapping in local energy sinks. At the same time dissipative interactions stabilize the initially created electronic excitations in lower-energy states on sub-ps time scales to create the ultrafast energy funnel to bottom B850 states and to prevent relaxation along competitive loss channels. Based on this reasoning it was predicted that comparable timescales for population transfer, dissipative relaxation and pure dephasing of coherence lead to the highest energy transfer efficiency in photosynthetic light-harvesting complexes.[52] The coupling constants and decoherence times found in our study are indeed comparable and seem optimized for individual light harvesting complexes, suggesting that coherence plays an important role in efficient energy transfer.[23]

7. Discussion and reflection

When combining femtosecond spectroscopy with detection of individual molecules, one often runs into a difference in jargon between femtosecond spectroscopists and single molecule spectroscopists. A significant fraction of this difference finds its origin in the "regime" in which the experiments take place, specifically the intensity with which one excites the molecule. Terms that are often used interchangeably are "non-saturating" and "saturating"; "linear" and "non-linear"; "weak-field" and "strong-field", with discussion focussing on questions like the nature of "coherent control" when in the "weak-field" regime, the meaning of "phase" and "coherent" when the interaction is "linear", what the relation is between "linearity" and "saturation" and what exactly is meant by "non-linear" in a certain context.

"Weak-field" and "strong-field" were not used in this review since especially "strong-field" as a term has largely been adopted by the attosecond community to mean a significant interaction between the electron orbital of an atom/molecule and an impinging electric field, within one oscillation of the electric field. In contrast, "weak-field" has been used to signify the regime in which the interaction between the molecular dipole and the electric field is weak enough as to not cause Rabi-oscillations. The regimes are two extremes on a

continuum of increasing intensity. Our experiments morph quite naturally from 'weak-field' into 'strong field' depending on the orientation of the molecule in the sample, *i.e.* the overlap between the excitation dipole and the incident electric field, as shown in *e.g.* Fig. 7. It therefore makes little sense to make a hard statement about the "regime" in which these experiments take place.

The same largely holds for the other terms. In the picture posited above, "saturation" would mean an intensity so high that the molecule undergoes fast oscillation between ground and excited states, without an increase in intensity significantly increasing the excited state population probability. In pulsed experiments this explanation of the term lacks clarity, but in the same vein as weak-field and strong-field, it can easily be explained in terms of the Bloch vector and Rabi oscillations, where "saturating" would then simply mean having a Rabi-frequency significantly higher than the decoherence rate, and "non-saturating" the opposite.

"Linear" and "nonlinear" have the added complication that both terms can be used in two different ways: they can mean the same as "weak-field" and "strong-field" above, or they can be used to signify an interaction with one, *vs.* multiple photons. This is a subtle difference, but it would be possible to *e.g.* have a 1-photon interaction in the strong field regime, or a 2-photon interaction in the weak-field regime and have both be described as either "linear" or "non-linear".

We have therefore opted to consistently adopt a semi-classical picture in which the interaction with light is described in terms of fields (where every interaction with either "one" or "multiple" photons is probabilistic), and we have tried to avoid the terms "linear" and "non-linear". Since the strong-field association with attoscience is quite influential, we also chose not to use "weak-field" and "strong-field", and have opted for the terms "saturating" or "non-saturating" when we needed to delineate the two extremes of interaction between the molecule and the electromagnetic field.

A consistent application of the semi-classical picture used throughout in this review supplies a model that naturally encompasses all dynamics observed in our experiments. However, the discussion of "regime" of the experiment often leads to other questions pertaining to coherence and phase, observed and induced coherence, and the distinguishability of different types of couplings and coherences in molecules. Below, we will discuss some of these issues.

Time *vs.* frequency domain description and the role of the spectral phase

From a purely theoretical view-point, measurements in the time domain and in the frequency domain can be thought to be equivalent, straightforwardly linked through the Fourier transformation. It is true that ultrafast pulses can be described both in the time-domain and frequency domain without loss of information. In a naïve fashion, this could lead one to believe that pulse shaping experiments yield results equivalent to those that can be obtained using tuneable CW lasers. Yet this notion ignores the most important aspect of the spectral description of

ultrafast pulses: the spectral phase. Generally speaking, it is therefore impossible to describe the results of ultrafast experiments in terms of CW spectroscopy: the spectral phase is an integral part of the experiment and determines the dynamics induced in molecules using ultrashort pulses.

In fact to consider an experiment with pulses equivalent to an experiment with tuneable CW light, one has to meet very strict conditions: (1) the experiment is performed in the "non-saturating" (*i.e.* linear, weak-field *etc.*) regime, (2) only Fourier limited pulses are used (*i.e.* all shaping is amplitude shaping and the spectral phase is flat throughout), (3) the experiment is not limited by the amount of read-out photons available. Only in this limiting case, an experiment with ultrafast pulses can be thought of as spectroscopy in a different set of bases. Note that condition (3) is vital here, since the only way in which these two experiments contain the same information is when both have enough readout photons to encompass the entire time (frequency) space. However, these conditions are typically not imposed on ultrafast experiments and are certainly never met in single molecule experiments, where even if conditions (1) and (2) are met, the limited amount of photocycles available before photobleaching will ensure that a time domain experiment would result in a complementary dataset to a frequency domain experiment.

Phrased differently, this also shows the richness of ultrafast experiments compared to CW experiments; a description in the frequency domain shows that with tuneable CW lasers, spectral amplitude is the only accessible parameter, whereas with ultrafast pulse shaping, both spectral amplitude and phase are independently addressable. This changes the experiment from taking place in a 1D parameter space to a 2D parameter space and leads to proportionally more access to information.

Electronic *vs.* vibrational coherence; coherence in the site basis *vs.* coherence in the exciton basis

In pump probe experiments, as described in Sections 4, 5 and 6, one induces a coherent superposition with the first pulse, to be probed with the second pulse. Typically this probes coherence in the exciton basis, *i.e.* between eigen-states of a quantum system, indicative of quantum dynamics in the system under investigation induced by interaction with coherent light. The coherence can be both vibrational and electronic; it depends on the system in question, the selected pump and probe wavelengths, and the signal observed, which is being probed. For instance, in the experiments in Section 4, only an electronic ground state and an electronic excited state were involved, and the response measured (Fig. 7) is indicative of the decay of electronic coherence. In Section 5, a degenerate broadband pump probe experiment was performed, where the fast oscillations were indicative of vibrational coherence, while the decaying envelope around the oscillations is again the decay of electronic coherence (Fig. 10).

Using the two colour method described in Section 6, a coherent contribution to the energy transfer between B800 and B850, mediated by electronic coupling, was measured in LH2. Although it is a matter of theoretical debate whether the

method presented there is also suited to probe vibrational coherence, the oscillations in Fig. 11C can confidently be attributed to electronic coherence: any vibrational signal would have to stem from Franck–Condon active, *i.e.* optically accessible, vibrations. LH2 has been extensively analysed in steady state spectroscopy, both at cryogenic and biological temperatures, and no vibrational mode with an energy corresponding to the 200 fs period we measured has been identified to couple to the electronic transition. Conversely, this period could be described by an electronic B800–B850 coupling constant $J = 50$ cm^{-1} which is well in the range of values measured over the years. In other words, here we measured electronic coherence between electronically excited eigenstates of the LH2 complex, that is induced by the coupling J and not by specific excitation conditions. As such this is an intrinsic property of the molecular assembly. This constitutes a fundamentally different situation from the (much shorter lived) ground – excited state electronic coherence described in Section 4 and the vibrational wave packets in Section 5, which can only be created by a specific excitation with an external field.

To conclude, the coherence measured in molecular systems can be both of vibrational and electronic nature; which is probed depends on the system in question, the selected pump and probe wavelengths, *i.e.* the molecular levels involved, the spectral bandwidths of pump and probe pulses, and possible (electronic) interactions between chromophores within an assembly.

8. Conclusions

We have presented an overview of recent advances in the detection of ultrafast dynamics of single molecules. Examples on electronic coherence, vibrational wave-packet interference, vibrational relaxation decay and coherent electronic energy transfer, illustrate the versatility of the technology. Most importantly single (bio)molecules in their natural ambient condition can be addressed which is crucial for applications in biology and molecular photonics. Particularly the detection of persistent coherences in individual light harvesting complexes provides an unprecedented look into the functioning of photosynthetic energy transfer, with guidelines for efficient energy flow through molecular systems.

Probably the main conclusion that can be drawn from this set of investigations is that coherence, both induced and intrinsic, is relevant to the interaction of light with complex molecules and molecular assemblies at room temperature. Single molecule experiments greatly facilitate the observation of coherent effects in complex systems under these conditions. On a fundamental level, they provide the opportunity to investigate molecular dynamics under conditions previously unattainable; they allow observing of quantum mechanics "at work" in everyday circumstances; and they shed light on the (quantum) physics underlying heavily evolved molecular systems. It is important to realize that, due to intermolecular heterogeneity, single molecule experiments provide a realistic look of the coherence times in each unit; bulk experiments would tend

to underestimate coherence times due to inhomogeneous averaging. Equally important is realizing that the ergodicity principle (*i.e.* time-averaging equals ensemble averaging) does not hold for investigations on systems in functional interaction with a structured environment, and for measurements based on limited photocounts and observation times. As such, while bulk experiments are indispensable for calibrating *structurally* determined responses of complex molecular systems, single molecule research provides an approach to discover the *functional* characteristics of complex molecules. Further femtosecond single molecule investigations like the ones presented here, in combination with theoretical calculations, have the potential to resolve the dynamics and photophysics of complex molecular systems previously out of reach of physical study.

All schemes presented here rely on fluorescence detection. Many interesting systems do fluoresce and can be studied on a fs time scale, yet the dependence on fluorescence comes with rapid photo-reaction and blinking, both of which complicate long term systematic observations. Thus it remains important to endeavour for alternative detection schemes such as absorption, stimulated emission, Raman scattering or enhancement by nanoantennas. Hopefully, in the near future, fs spectroscopy with single molecule sensitivity will form part of the extensive palette of molecular spectroscopic methodologies.

Acknowledgements

References

1 W. E. Moerner and L. Kador, Optical detection and spectroscopy of single molecules in a solid, *Phys. Rev. Lett.*, 1989, **62**, 2535.

2 M. Orrit and J. Bernard, Single pentacene molecules detected by fluorescence excitation in a *p*-terphenyl crystal, *Phys. Rev. Lett.*, 1990, **65**, 2716–2719.

14 | *Chem. Soc. Rev.*, 2014, **00**, 1–16

This journal is © The Royal Society of Chemistry 2014

3 W. E. Moerner and M. Orrit, *Science*, 1999, **283**, 1670.

4 W. P. Tamarat, A. Maali, B. Lounis and M. Orrit, *J. Phys. Chem. A*, 2000, **104**, 1; W. E. Moerner, *J. Phys. Chem. B*, 2002, **106**, 910.

5 A. Yildiz, J. N. Forkey, S. A. McKinney, T. Ha, Y. E. Goldman and P. R. Selvin, *Science*, 2003, **300**, 2061.

6 J. J. Macklin, J. K. Trautman, T. D. Harris and L. E. Brus, *Science*, 1996, **272**, 255.

7 J. A. Veerman, M. F. Garcia-Parajo, L. Kuipers and N. F. van Hulst, *Phys. Rev. Lett.*, 1999, **83**, 2155.

8 K. D. Weston, P. J. Carson, H. Metiu and S. K. Buratto, *J. Chem. Phys.*, 1998, **109**, 7474.

9 R. A. L. Vallée, N. Tomczak, L. Kuipers, G. J. Vancso and N. F. van Hulst, *Phys. Rev. Lett.*, 2003, **91**, 38301.

10 X. S. Xie and J. K. Trautman, *Annu. Rev. Phys. Chem.*, 1998, **49**, 441.

11 G. S. Engel, T. R. Calhoun, E. L. Read, T.-K. Ahn, T. Mancal, Y.-C. Cheng, R. E. Blankenship and G. R. Fleming, Evidence for wavelike energy transfer through quantum coherence in photosynthetic systems, *Nature*, 2007, **446**(7137), 782–786.

12 E. Collini, C. Y. Wong, K. E. Wilk, P. M. G. Curmi, P. Brumer and G. D. Scholes, Coherently wired light-harvesting in photosynthetic marine algae at ambient temperature, *Nature*, 2010, **463**(7281), 644–647.

13 T. Guenther, C. Lienau, T. Elsaesser, M. Glanemann, V. M. Axt, T. Kuhn, S. Eshlaghi and A. D. Wieck, *Phys. Rev. Lett.*, 2002, **89**, 057401; T. Unold, K. Mueller, C. Lienau, T. Elsaesser and A. D. Wieck, *Phys. Rev. Lett.*, 2004, **92**, 157401.

14 V. Westphal, L. Kastrup and S. W. Hell, *Appl. Phys. B: Lasers Opt.*, 2003, **77**, 377.

15 M. Dyba and S. Hell, *Phys. Rev. Lett.*, 2002, **88**, 163901.

16 L. Kastrup and S. Hell, *Angew. Chem., Int. Ed.*, 2004, **43**, 6646.

17 E. M. H. P. van Dijk, J. Hernando, J. J. García-López, M. Crego-Calama, D. N. Reinhoudt, L. Kuipers, M. F. García-Parajó and N. F. van Hulst, Single molecule pump–probe detection resolves ultrafast pathways in individual and coupled quantum systems, *Phys. Rev. Lett.*, 2005, **94**, 78302.

18 E. M. H. P. van Dijk, J. Hernando, M. F. García-Parajó and N. F. van Hulst, Single-molecule pump–probe experiments reveal variations in ultrafast energy redistribution, *J. Chem. Phys.*, 2005, **123**, 64703.

19 J. Hernando, E. M. H. P. van Dijk, J. P. Hoogenboom, J. J. García-López, M. Crego-Calama, D. N. Reinhoudt, M. F. García-Parajó and N. F. van Hulst, Effect of disorder on ultrafast exciton dynamics probed by single molecule spectroscopy, *Phys. Rev. Lett.*, 2006, **97**, 216403.

20 R. Hildner, D. Brinks, F. D. Stefani and N. F. van Hulst, Electronic coherences and vibrational wave-packets in single molecules studied with femtosecond phase-controlled spectroscopy, *Phys. Chem. Chem. Phys.*, 2011, **13**, 1888–1894.

21 D. Brinks, F. D. Stefani, F. Kulzer, R. Hildner, T. H. Taminiau, Y. Avlasevich, K. Müllen and N. F. van Hulst, Visualizing and controlling vibrational wave packets of single molecules, *Nature*, 2010, **465**(7300), 905–908; D. Brinks, R. Hildner, F. D. Stefani and N. F. van Hulst, Coherent control of single molecules at room temperature, *Faraday Discuss.*, 2011, **153**, 51–60.

22 R. Hildner, D. Brinks and N. F. van Hulst, Femtosecond coherence and quantum control of single molecules at room temperature, *Nat. Phys.*, 2011, **7**, 172–177.

23 R. Hildner, D. Brinks, J. B. Nieder, R. J. Cogdell and N. F. van Hulst, *Science*, 2013, **340**, 1448–1451.

24 T. Brixner, *et al.*, Two-dimensional spectroscopy of electronic couplings in photosynthesis, *Nature*, 2005, **434**, 625.

25 G. Panitchayangkoon, *et al.*, Long-lived quantum coherence in photosynthetic complexes at physiological temperature, *Proc. Natl. Acad. Sci. U. S. A.*, 2010, **107**, 12766.

26 D. Hayes, G. B. Griffin and G. S. Engel, Engineering coherence among excited states in synthetic heterodimer systems, *Science*, 2013, **340**, 1431–1434.

27 S. Chong, W. Min and X. S. Xie, Ground-state depletion microscopy: detection sensitivity of single-molecule optical absorption at room temperature, *J. Phys. Chem. Lett.*, 2010, **1**, 3316–3322.

28 P. Kukura, M. Celebrano, A. Renn and V. Sandoghdar, Single-molecule sensitivity in optical absorption at room temperature, *J. Phys. Chem. Lett.*, 2010, **1**, 3323–3327.

29 M. Celebrano, P. Kukura, A. Renn and V. Sandoghdar, Single-molecule imaging by optical absorption, *Nat. Photonics*, 2011, **5**, 95–98.

30 A. Gaiduk, M. Yorulmaz, P. V. Ruijgrok and M. Orrit, Room-temperature detection of a single molecule's absorption by photothermal contrast, *Science*, 2010, **330**, 353–356.

31 S. Nie and S. R. Emory, Probing single molecules and single nanoparticles by surface-enhanced Raman scattering, *Science*, 1997, **275**, 1102–1106.

32 W. Min, C. W. Freudiger, S. Lu and X. S. Xie, Coherent nonlinear optical imaging: beyond fluorescence microscopy, *Annu. Rev. Phys. Chem.*, 2011, **62**, 507–530.

33 M. J. Winterhalder, A. Zumbusch, M. Lippitz and M. Orrit, *J. Phys. Chem. B*, 2011, **115**, 5425–5430.

34 W. Min, *et al.*, Imaging chromophores with undetectable fluorescence by stimulated emission microscopy, *Nature*, 2009, **461**, 1105–1109.

35 M. J. Rosker, F. W. Wise and C. L. Tang, Femtosecond relaxation dynamics of large molecules, *Phys. Rev. Lett.*, 1986, **57**, 321–324.

36 D. J. Nesbitt and R. W. Field, Vibrational energy flow in highly excited molecules: role of intramolecular vibrational redistribution, *J. Phys. Chem.*, 1996, **100**, 12735–12756.

37 T. Kasajima, S. Akimoto, S. Sato and I. Yamazaki, Vibrational energy relaxation of S_1 perylene in solution, *J. Phys. Chem. A*, 2004, **108**, 3268–3275; IVR: T. Kiba, S. Sato, S. Akimoto, T. Kasajima and I. Yamazaki, Solvent-assisted intramolecular vibrational energy redistribution of S_1 perylene in ketone solvents, *J. Photochem. Photobiol., A*, 2006, **178**, 201–207.

38 J. Hofkens, T. Vosch, M. Maus, F. KÄohn, M. Cotlet, T. Weil, A. Herrmann, K. Müllen and F. C. De Schryver, *Chem. Phys. Lett.*, 2001, **333**, 255.

39 Y. Silberberg and D. Meshulach, Coherent quantum control of two-photon transitions by a femtosecond laser pulse, *Nature*, 1998, **396**(6708), 239–242; H. Rabitz, R. de Vivie-Riedle, M. Motzkus and K. Kompa, Whither the future of controlling quantum phenomena? *Science*, 2000, **288**(5467), 824–828.

40 J. L. Herek, W. Wohlleben, R. J. Cogdell, D. Zeidler and M. Motzkus, Quantum control of energy flow in light harvesting, *Nature*, 2002, **417**(6888), 533–535.

41 V. I. Prokhorenko, A. M. Nagy, S. A. Waschuk, L. S. Brown, R. R. Birge and R. J. D. Miller, Coherent control of retinal isomerization in bacteriorhodopsin, *Science*, 2006, **313**(5791), 1257–1261.

42 D. G. Kuroda, C. P. Singh, Z. Peng and V. D. Kleiman, Mapping excited-state dynamics by coherent control of a dendrimer's photoemission efficiency, *Science*, 2009, **326**(5950), 263–267.

43 M. Aeschlimann, M. Bauer, D. Bayer, T. Brixner, F. J. García de Abajo, W. Pfeiffer, M. Rohmer, C. Spindler and F. Steeb, Adaptive subwavelength control of nano-optical fields, *Nature*, 2007, **446**(7133), 301–304; M. Aeschlimann, *et al.*, Coherent two-dimensional nanoscopy, *Science*, 2011, **333**, 1723–1726.

44 D. Brinks, M. Castro-Lopez, R. Hildner and N. F. van Hulst, Plasmonic antennas as design elements for coherent ultra-fast nanophotonics, *Proc. Natl. Acad. Sci. U. S. A.*, 2013, **110**, 18386–18390.

45 Y. S. Avlasevich, *et al.*, Novel core-expanded rylenebis-(dicarboximide) dyes bearing pentacene units: facile synthesis and photophysical properties, *Chem.–Eur. J.*, 2007, **13**, 6555–6561.

46 V. V. Lozovoy, I. Pastirk and M. Dantus, Multiphoton intrapulse interference (MIIPS); Characterization and compensation of the spectral phase of ultrashort laser pulses, *Opt. Lett.*, 2004, **29**, 775–777.

47 D. Brinks, R. Hildner, F. D. Stefani and N. F. van Hulst, Beating spatio-temporal coupling: implications for pulse shaping and coherent control experiments, *Opt. Express*, 2011, **19**, 26486; N. Accanto, J. B. Nieder, L. Piatkowski, M. Castro-Lopez, F. Pastorelli, D. Brinks and N. F. van Hulst, Phase control of femtosecond pulses on the nanoscale using second harmonic nanoparticles, *Light: Sci. Appl.*, [Q7] 2014, accepted [arXiv:1305.3783, 2013].

48 M. A. Bopp, A. Sytnik, T. D. Howard, R. J. Cogdell and R. M. Hochstrasser, The dynamics of structural deformations of immobilized single light-harvesting complexes, *Proc. Natl. Acad. Sci. U. S. A.*, 1999, **96**, 11271.

49 A. M. van Oijen, M. Ketelaars, J. Kohler, T. J. Aartsma and J. Schmidt, Unraveling the electronic structure of individual photosynthetic pigment–protein complexes, *Science*, 1999, **285**, 400; C. Hofmann, M. Ketelaars, M. Matsushita, H. Michel, T. J. Aartsma and J. Kohler, *Phys. Rev. Lett.*, 2003, **90**, 013004.

50 G. S. Schlau-Cohen, Q. Wang, J. Southall, R. J. Cogdell and W. E. Moerner, Single-molecule spectroscopy reveals photosynthetic LH2 complexes switch between emissive states, *Proc. Natl. Acad. Sci. U. S. A.*, 2013, **110**(27), 10899–10903.

51 E. Harel and G. S. Engel, Quantum coherence spectroscopy reveals complex dynamics in bacterial light-harvesting complex 2 (LH2), *Proc. Natl. Acad. Sci. U. S. A.*, 2012, **109**, 706.

52 P. Rebentrost, M. Mohseni, I. Kassal, S. Lloyd and A. Aspuru-Guzik, *New J. Phys.*, 2009, **11**, 033003; M. B. Plenio and S. F. Huelga, *New J. Phys.*, 2008, **10**, 113019; M. Mohseni, P. Rebentrost, S. Lloyd and A. Aspuru-Guzik, *J. Chem. Phys.*, 2008, **129**, 174106.